

Quasi-static Modeling of Feeding Behavior in *Aplysia Californica*

Bidisha Kundu^(⊠), Stephen M. Rogers, and Gregory P. Sutton

School of Life Sciences, University of Lincoln, Lincoln LN6 7TS, UK {bkundu,sterogers}@lincoln.ac.uk, RScealai@gmail.com

Abstract. Behaviors that are produced solely through geometrically complex three-dimensional interactions of soft-tissue muscular elements, and which do not move rigid articulated skeletal elements, are a challenge to mechanically model. This complexity often leads to simulations requiring substantial computational time. We discuss how using a quasistatic approach can greatly reduce the computational time required to model slow-moving soft-tissue structures, and then demonstrate our technique using the biomechanics of feeding behavior by the marine mollusc, Aplysia californica. We used a conventional 2nd order (from Newton's equations), forward dynamic model, which required 14s to simulate 1s of feeding behavior. We then used a quasi-static reformulation of the same model, which only required 0.35s to perform the same task (a 40fold improvement in computation speed). Lastly, we re-coded the quasistatic model in Python to further increase computation speed another 3-fold, creating a model that required just 0.12s to model 1s of feeding behavior. Both quasi-static models produce results that are nearly indistinguishable from the original 2nd order model, showing that quasistatic formulations can greatly increase the computation speed without sacrificing model accuracy.

Keywords: Aplysia Californica · Biomechanics · Equilibrium point

1 Introduction

Understanding the neural control of behavior requires understanding both the nervous system and the muscles that it controls [1]. This often is facilitated by combining models of the nervous system [5] with forward kinetic models of the body [16]. A widely used model for such research has been the feeding apparatus of the marine mollusc, *Aplysia californica*, which has an experimentally tractable nervous system, composed of relatively few, large neurons, combined with a musculature that is easily experimented upon. These features have made

This work was funded by UKRI Grant Number (MR/T046619/1), part of the NSF/CIHR/DFG/FRQ/UKRI-MRC Next Generation Networks for Neuroscience Program. Also, there was additional supports to G.P.S. provided by the Royal Society (UF130507) and US Army Research Office (W911NF-15-038).

[©] The Author(s), under exclusive license to Springer Nature Switzerland AG 2022 A. Hunt et al. (Eds.): Living Machines 2022, LNAI 13548, pp. 80–90, 2022. https://doi.org/10.1007/978-3-031-20470-8_8

it a frequently used model system for the study of neural control [4]. Computer models of complex systems can greatly assist in understanding their fundamental properties, but a problem has arisen because of a major difference in the simulation times required to run models of neuronal function compared to those simulating the musculature: for example, the neuronal models of Li et al. [6] and Webster-Wood et al. [14] require 0.1s of computation time to simulate 1s of activity. In contrast, a commensurate model of the biomechanics of the buccal mass [12] requires 14s of computation time to simulate the mechanics of that 1s of behavior. These large computational requirements of the mechanical models have provided a substantial impediment to any research that involves evolutionary algorithms, machine learning, or any iterative technique that require running models large numbers of times. We have refined the 2nd order kinetic biomechanical model of [12] into a 0th order quasi-static form by using an algebraic reformulation, which reduces the computational time of the model by over 40 fold, thus making the entire model more compatible for research techniques that require large numbers of iterations. This algebraic reformulation technique is applicable for any slow-moving system.

Our biomechanical model system is the feeding apparatus of the marine mollusc, Aplysia californica [2,12]. This feeding apparatus is called 'the buccal mass', and has four key anatomical components. First, there is a spherical grasping structure, the "radula odontophore", which is moved toward the mouth (protraction), grasps food, and then moves back toward the esophagus (retraction) to deposit food (hereafter referred to as the 'odontophore'). Second, there is a sheet of muscle, the "I2", posterior to the odontophore, which, when activated, moves the odontophore forward. Third, there is a large circular muscle anterior to the odontophore, the "I3", which squeezes around the circumference of the odontophore. And fourth, there is a muscular structure called "the hinge" which anchors the ventral-most part of the odontophore to the surrounding tissue of the head. This acts to pull the odontophore back toward the esophagus. These four parts of the buccal mass were modeled using a 2nd order Newtonian formulation in [12].

2 Model

We have re-formulated the kinetic model of [12]. In this model [12], the four components of the Aplysia buccal mass are modeled as follows (Fig. 1): (1) odon-tophore is a sphere, (2) the I2 muscle is a sheet posterior to the odontophore, (3) the I3 muscle is a torus through which the odontophore passes and which can deliver either a forward or backwards force depending on the odontophore's position, and (4) the hinge is an elastic attachment connecting the odontophore to an external anchor. These three forcing agents generate the main forces in translation on the odontophore for grasping food and passing it back to the esophagus. The tensions in the I2 and I3 muscles are modeled as Hill type muscles with non-linear activation [10,12,15] with identical parameters as [12]. The hinge is modeled using both Maxwell and Kelvin visco-elastic elements in paral-

lel, following the method of [11,12]. The complete mechanical system is shown schematically in Fig.1.

2.1 Odontophore and I2, I3 Muscles

The odontophore is represented by a sphere of radius R, with mass M. The I2 muscle lies posterior to the odontophore and is modeled as hemispherical object with sheet-like extensions Fig. 1(b). In the 2D cross-sectional view Fig.(1a), the I2 muscle is the combination of AH (sheet like structure), HH' (hemispherical part), and H'A' (sheet like structure). I3 muscle is modeled as a torus anterior to I2 with mass m and cross-sectional radius r (see Fig. 1).

2.2 Assumptions

The center of the toroidal muscle I3 is the origin O of our coordinate system. The horizontal (anterior-posterior) direction is the X axis, and the Y axis is orthogonal to this passing through O. The location center of the odontophore, E, is constrained to move only along the X axis Fig. 1. The mechanics of the rest of the system are subsequently derived from the following assumptions.

- The I3 torus volume is constant, i.e., $V = 2\pi^2 y(t)r^2(t) = Constant$
- All the muscles and the odontophore remain in contact throughout. Contact condition: $x^2(t) + y^2(t) = (R + r(t))^2$
- The line AG connecting the center G of the minor radius of the torus and the contact point A of the I2 muscle to the I3 muscle is always parallel to X axis.

The force from I2 and the hinge both act directly on the odontophore, moving it horizontally, and thus these two forces can be summed (the sum of these forces will be referred to as ' F_1 ' in the subsequent equation of motion). The constraint on I3's position causes force from the I3 to act vertically, with the angle of contact (θ) between the I3 and the odontophore acting to mediate the resultant force. Consequently, the I3 force on the odontophore is calculated independently and called ' F_2 '.

2.3 Governing Equations

This geometry leads to the fundamental equation of motion for the entire system (Eq. 1), from [12], Eq. 3 we have

$$(m\ddot{y} + F_2)\cos(\theta) = (M\ddot{x} - F_1)\sin(\theta) \tag{1}$$

where F_1 is the force on the odontophore caused by I2 and the hinge, while F_2 is the force on the odontophore caused by I3. $F_1(x,t)$ and $F_2(x,t)$ can be solved in terms of the muscle geometry: θ, y, x , and r are then calculated for the each timestep, which then yields the linear acceleration of the odontophore, \ddot{x} . The acceleration is then integrated twice to calculate the position of the odontophore, x(t). Details and full model can be found in [12].

2.4 Reformulation

In simulations of buccal mass feeding behavior [12], the majority of the mechanical energy generated by the muscles is stored by elastic and visco-elastic elements of the hinge.

The kinetic energy $(\frac{1}{2} \text{ mass} \times \text{velocity}^2)$ due to the motion of the system is very low, with a maximum value of 2.66703×10^{-8} J. The dissipation of energy due to viscous fluid drag surrounding the odontophore $(\frac{1}{2} \text{ Coefficient of drag} \times \text{density of water} \times (\text{velocity})^2 \times \text{area} \times \text{displacement})$ is, at most, 4.13178×10^{-9} J. In contrast, the elastic energy of the system $(\frac{1}{2} \text{ elastic constant} \times \text{displacement}^2)$ has a maximum of 5.50×10^{-4} J, over 4 orders of magnitude higher than the kinetic energy or viscous damping (parameters taken from [12]). Less than 0.1% of the energy in the system is kinetic or dissipated by damping (damping coefficient \times velocity \times displacement). We thus propose the following reformulation of (Eq. 1), where we approximate \ddot{x} and \ddot{y} with 0. This is an example of a 'quasi-static' approximation [7–9] - and reduces the 2^{nd} order differential equation to a much simpler equation of static equilibrium (Eq. 2):

$$0 = F_2 Cot(\theta) + F_1 \tag{2}$$

Within the expressions of F_1 and F_2 , however, there are velocity dependent terms for the Force-Velocity properties of the I2 and the I3 muscles [12,16], which do affect the elastic energy in the system and thus cannot be removed. To show where these velocity terms occur, we expand Eq. (2) as follows

$$2\pi T_{I2}(x, y, \dot{x}, r, activation)Cos(\phi) + 2\pi T_{I3}(x, y, \dot{x}, r, activation)Cot(\theta) - Hingeforce = 0$$
 (3)

where T_{I2} and T_{I3} are the muscle tensions for the I2 and I3 muscles, respectively and $\angle AHQ = \phi$ (Fig. 1).

We make one final substitution to bring these equations down to a zeroth order formulation. To produce a purely position-dependent equation (i.e., x, y, and r dependent only), the velocity terms (\dot{x}) are approximated at each timestep as $\dot{x} = \frac{x - x_{previous}}{\triangle t}$. Then Eq. (3) can be expressed as

$$2\pi T_{I2}(x,y,\frac{x-x_{previous}}{\triangle t},r,activation)Cos(\phi) + 2\pi T_{I3}(x,y,\frac{x-x_{previous}}{\triangle t},r,activation)Cot(\theta) - Hingeforce = 0. \eqno(4)$$

The equation of motion of the odontophore is Equation (4) with the added constraints that I3 is iso-volumetric ($V = 2\pi^2 y(t)r^2(t)$ =Constant) and that I3 must be in contact with the odontophore ($x^2 + y^2 = (R+r)^2$)). This produces a system where one variable (x) can be solved for its static equilibrium position.

At each time step we summed all of the forces that protracted the odontophore (positive), and all the forces that retracted the odontophore (negative), to find the equilibrium point where these forces are equal; i.e. the position where the sum of the forces on the odontophore is zero Fig. 2. The position of these equilibrium points varied as a function of muscle activation, and tracking the movement of these equilibrium points over time resulted in an approximation for odontophore position x. These equilibrium points were found numerically using Newton's method. In the Python formulation, these equations were solved using a Gauss-Newton algorithm with gradient descent (fsolve command) [13].

3 Results and Discussion

We simulated the complete 2nd order model [12] in Mathematica (Wolfram) [3] using the semi-implicit Euler method [14] for 60 s of odontophore motion. We set the initial position at t=0 as x=-5mm. At the beginning of the simulation the odontophore moves from its initial position to its resting equilibrium state. We activated I2 to protract the odontophore, and then let I2 relax, which resulted in a retraction of the odontophore Fig. 3. It required 14s of computer processing time to simulate 1s of behavior Fig. 3. Next, we simulated the same equations using our quasi-static formulation, which required only 0.13s of computer processing time to simulate 1s of behavior; a 107 times increase in computational speed Fig. 5. The results closely resemble results obtained from the original 2nd order formulation Fig. 3 with the maximum difference in position observed at the end of retraction Fig. 3c. This was the result of the rapid loss of muscle tension causing the odontophore to move at a relatively high velocity. There was a small temporal disparity between models, which translated into a brief spike of increased positional difference. The system time constant is 2.45 s [12] and this spike of discrepancy lasts for less than 0.01 s, which is too short a period for the muscles to react or change behavior.

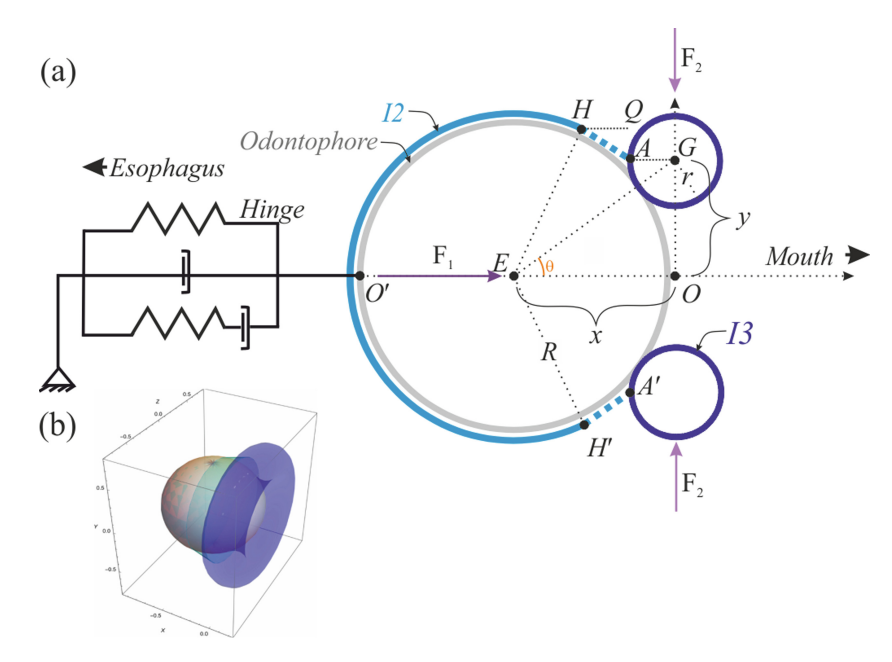


Fig. 1. a) Schematic figure of a 2D mid-sagittal view of the buccal mass system. Grey sphere, the odontophore; cyan, the I2 muscle comprised of hemispherical (solid line) and sheet-like (dotted line) elements; blue, section through the toroidal I3 muscle. The hinge is a passive elastic element anchoring the odontophore to the back of the head. See text for full details. b) Schematic 3D construction of the buccal mass: the odontophore (grey sphere) is surrounded by the hemispherical I2 muscle (cyan) which attaches anteriorly to the I3 ring muscle (blue). (Color figure online)

The majority of this computational speed increase (Fig. 5) was because the quasi-static formulation was numerically stable for step sizes of 0.01 s, while the 2nd order model required a step size of 0.0008 s. As the inertia term is present in the 2nd order model, it takes step size of 0.0008 s to accurately follow acceleration in the system. This step size is required because the mechanical resonant-frequency of the odontophore-hinge system is of the order 1000 Hz, requiring a very small step size to stably model it using the 2nd order system. This vibration is not biologically relevant to the system which is why the quasi-static model (which disregards this vibration) accurately reflects movements despite a much larger step size.

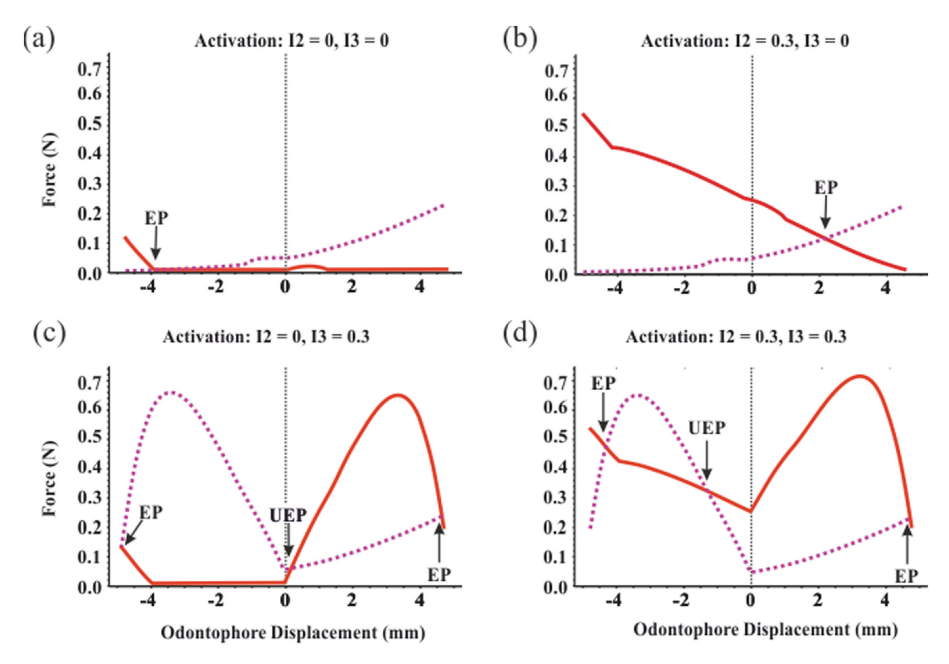


Fig. 2. The locations of equilibrium points, where the resultants of all the forces are zero. The red lines represent the positive and magenta dotted lines represent the negative parts of the resultant force. a) the profile of the forces when no muscles are active; passive forces within I2 and the hinge create a stable equilibrium point (EP) at an odontophore displacement of -4 mm. b) Profile of the forces when I2 is 30% activated. This results in a stable equilibrium point occurring at $+2 \,\mathrm{mm}$. c) Profile of the forces when I3 is 30% activated. This results in an unstable equilibrium point (UEP) at a displacement of 0 mm (the location at which the I3 is squeezing directly on the central axis of the odontophore). There is a stable equilibrium point at a displacement of +5 mm where I3 force is equal and opposite to the force of the hinge. There is a second a stable equilibrium point at -5 mm, where the I3 force is equal and opposite to the passive forces of I2. d) Profile of the forces when both I2 and I3 are 30% activated. There is an unstable equilibrium at a displacement of -1.5 mm, which occurs when the hinge and I3 forces are equal to the force of the active I2. There are two stable equilibrium points, one at $+5.5\,\mathrm{mm}$ where I3 and I2 forces are equal and opposite to the hinge, and at -4.5 mm where I3 force is equal and opposite to I2 force.

We simulated a second behavior where both I2 and I3 muscles were activated Fig. 4. The computation time for this simulation was the same as the simulation where only the I2 muscle was activated. As with the previous simulation, the quasi-static model and $2^{\rm nd}$ order model generated very similar output for odontophore position Fig. 4 with the quasi-static model requiring less than 5% of the computer processing time than the $2^{\rm nd}$ order model. This demonstrates that our quasi-static reformulation holds for more complex simulations of Aplysia feeding behavior.

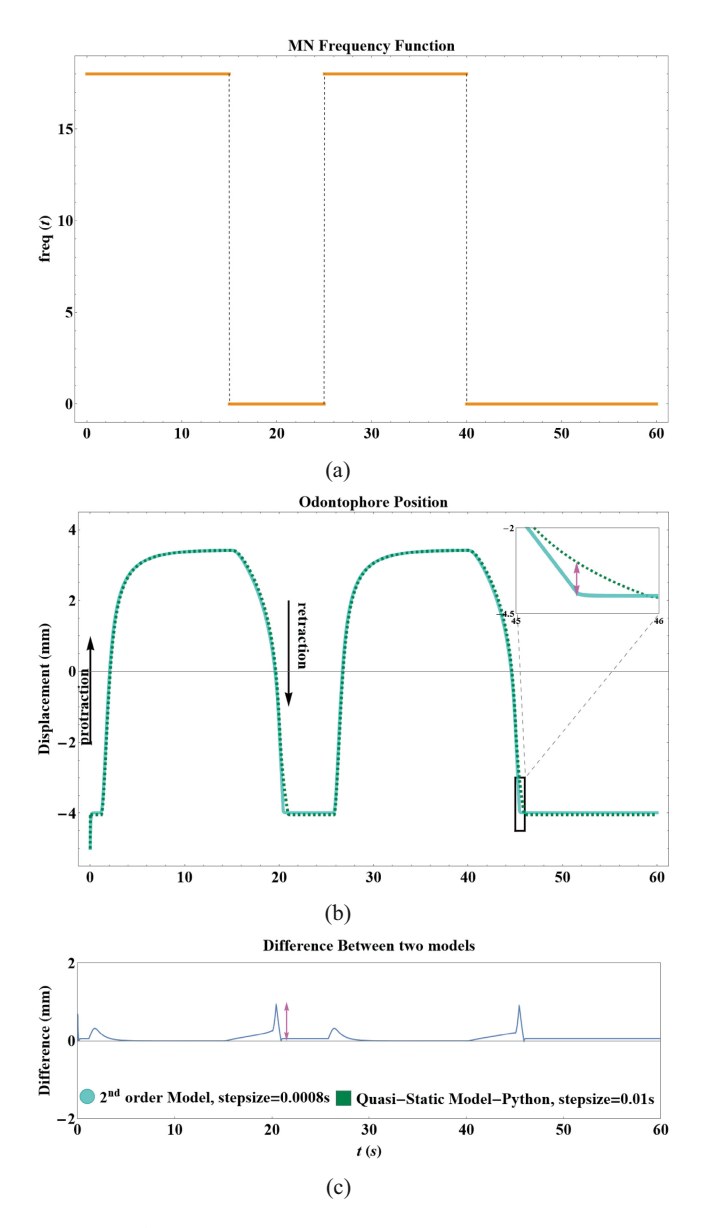


Fig. 3. Examples of $2^{\rm nd}$ order and quasi-static simulations of activating I2 within the buccal mass. a) Firing frequency function of motor neurons (MN) driving I2 where freq(t)=18 Hz for $0\,s\leq t\leq 15\,{\rm s}$, $25\,s\leq t\leq 40\,{\rm s}$ or otherwise 0. b) The resulting displacement of the odontophore (x) as simulated by the $2^{\rm nd}$ order (teal, solid line) and quasi-static (green, dotted line) models. The initial rapid displacement to $-4\,{\rm mm}$ at the beginning of the simulation corresponds to the stable equilibrium that arises from purely passive forces in the buccal mass as shown in Fig. 2a. (c) The difference between the numerical values of solution x using the two models. The inset in (b) shows a magnified-version of the difference in the time interval $[45\,{\rm s},\,46\,{\rm s}]$. (Color figure online)

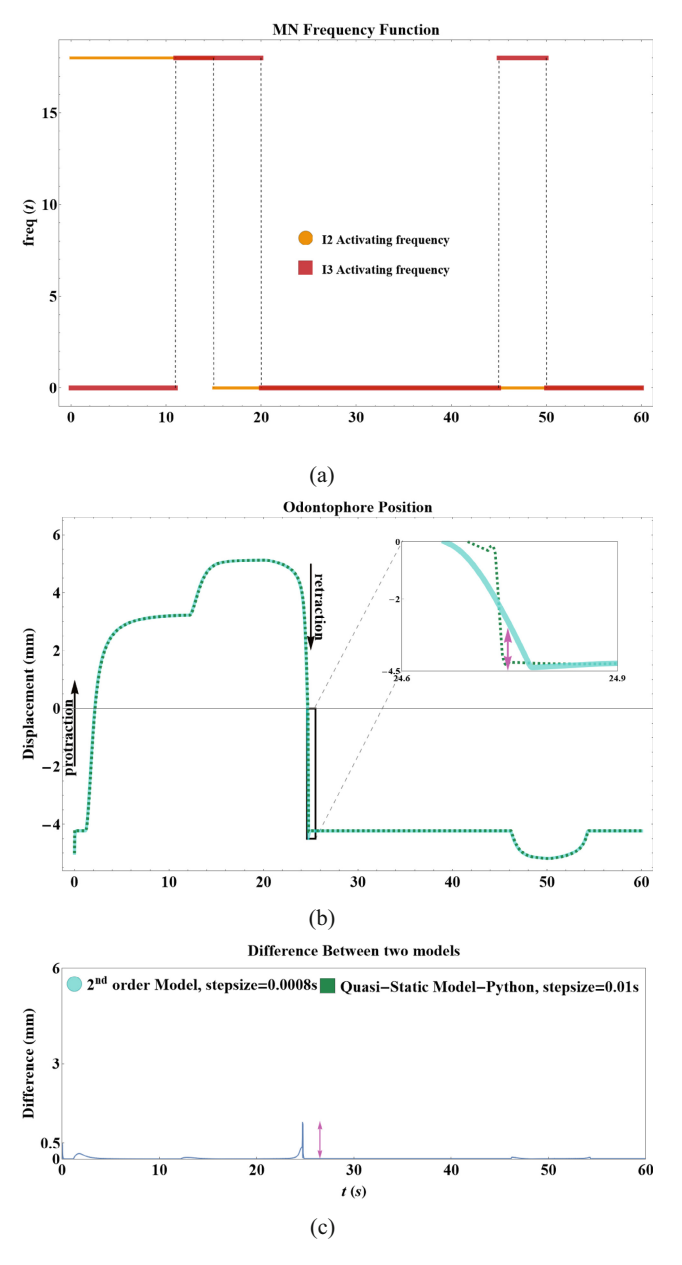


Fig. 4. Examples of $2^{\rm nd}$ order and quasi-static simulations of activating both I2 and I3 within the buccal mass. a) Firing frequency function of motor neurons (MN) driving I2 (orange) where freq(t)=18 Hz for $0s \le t \le 15 \, {\rm s}, \, 25 \, s \le t \le 40 \, {\rm s}$ or otherwise 0 and driving I3 (red) where freq(t)=18 Hz for $11s \le t \le 20 \, {\rm s}, \, 45 \, s \le t \le 50 \, {\rm s}$ or otherwise 0. b) The resulting displacement of the odontophore (x) as simulated by the $2^{\rm nd}$ order (teal, solid line) and quasi-static (green, dotted line) models. (c) The difference between the numerical values of solution x using the two models. The inset in (b) shows a magnified-version of the difference in the time interval $[24.6 \, {\rm s}, \, 24.9 \, {\rm s}]$. (Color figure online)

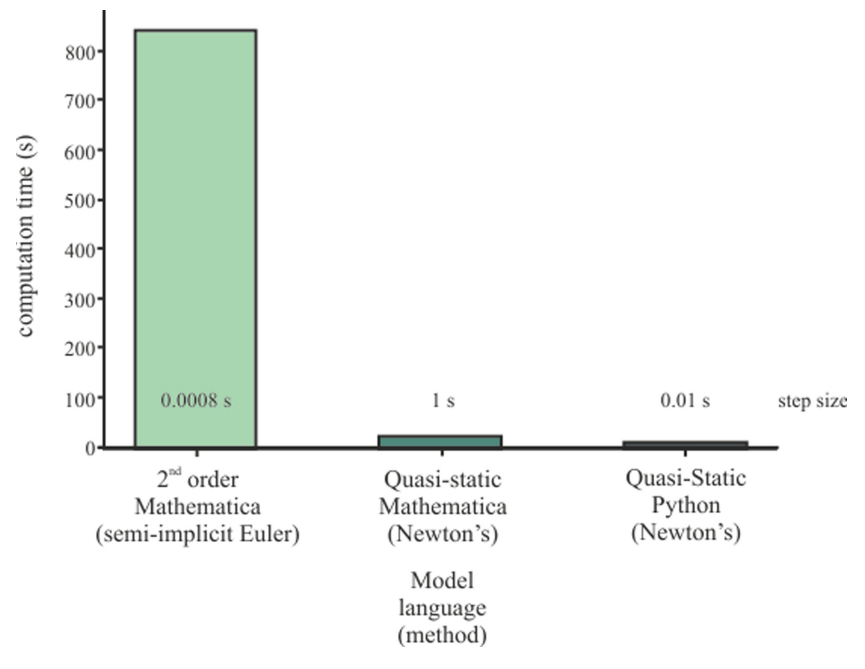


Fig. 5. Bar chart comparison of computation time of different models calculated using Mathematica and Python languages.

References

- Chiel, H.J., Beer, R.D.: The brain has a body: adaptive behavior emerges from interactions of nervous system, body and environment. Trends Neurosci. 20(12), 553–557 (1997)
- 2. Howells, H.: The structure and function of the alimentary canal of Aplysia punctata. J. Cell Sci. 2(331), 357–397 (1942)
- 3. Inc., W.R.: Mathematica, Version 13.1. Champaign (2022). https://www.wolfram.com/mathematica
- 4. Kandel, E.R.: Behavioral Biology of Aplysia. A Contribution to the Comparative Study of opisthobranch molluscs 463 (1979)
- Kandel, E.R., et al.: Principles of Neural Science, vol. 4. McGraw-hill, New York (2000)
- Li, Y., et al.: Using Synthetic Nervous Systems to Model the Multifunctional and Adaptive Feeding Behavior of Aplysia californica, vol. P962.02. Society for Neuroscience (2021)
- 7. Peshkin, M.A., Sanderson, A.C.: A variational Principle for Quasistatic Mechanics. Carnegie-Mellon University, Robotics Institute (1986)
- 8. Peshkin, M.A., Sanderson, A.C.: Minimization of energy in quasistatic manipulation. In: Proceedings. 1988 IEEE International Conference on Robotics and Automation, pp. 421–426. IEEE (1988)
- Ruina, A.L.: Friction laws and instabilities: a quasistatic analysis of some dry frictional behavior. Ph.D. thesis, Brown University (1981)

- Snyder, V.A.: Analysis of the biomechanics and neural control of two kinetic models of the buccal mass of Aplysia. Case Western Reserve University (Health Sciences) (2005), https://www.proquest.com/docview/305390183/ abstract/B303E6FBC4924763PQ/1
- Sutton, G.P., et al.: Passive hinge forces in the feeding apparatus of Aplysia aid retraction during biting but not during swallowing. J. Comp. Physiol. A 190(6), 501–514 (2004)
- 12. Sutton, G.P., et al.: Neural control exploits changing mechanical advantage and context dependence to generate different feeding responses in Aplysia. Biol. Cybern. 91(5), 333–345 (2004)
- 13. Virtanen, P., et al.: SciPy 1.0 Contributors: SciPy 1.0: fundamental algorithms for scientific computing in python. Nat. Methods 17, 261–272 (2020). https://doi.org/10.1038/s41592-019-0686-2
- Webster-Wood, et al.: Control for multifunctionality: bioinspired control based on feeding in Aplysia californica. Biol. Cybern. 114(6), 557–588 (2020)
- 15. Yu, S.N., et al.: Biomechanical properties and a kinetic simulation model of the smooth muscle I2 in the buccal mass of Aplysia. Biol. Cybern. **81**(5), 505–513 (1999)
- 16. Zajac, F.E.: Muscle and tendon: properties, models, scaling, and application to biomechanics and motor control. Crit. Rev. Biomed. Eng. 17(4), 359–411 (1989)